Holography

Review on Computer Generated Holography and Simulation with SLM

Gonçalo Ribeiro, Manuel Ratola, Margarida Pereira*
Instituto Superior Técnico, Physics Department, Lisboa, Portugal
(Dated: November 2023 - January 2024)

This article is centered on holography and its applications in beam shaping and image reconstruction using phase-only changing devices (i.e. Spatial Light Modulator - SLM). Firstly, holography is introduced, presenting its principles, state-of-the-art, and applications. Secondly, different methods used in Computer Generated Holography are also discussed, including the use of AI in SLM. Finally, after implementing a simulation code in Python, a vortex beam was generated using a Gaussian Beam, and the Gerchbert-Saxton algorithm was also implemented for image reconstruction.

I. INTRODUCTION

A. History

In 1947, Gabor introduced the concept of holography while attempting to improve the resolving power of the electron microscope and coined the term **hologram** [1]. Holography's principle consists of transforming phase shifts into an interference pattern - with it, a hologram records a phase and an amplitude [2, 3]. However, at the time, sources of coherent light were not available, thus it was not possible to explore the full potential of holography. It wasn't until 1963 when Leith and Upatnieks introduced the laser [1] to holography [1], opening the door to a large variety of applications due to the possibility of producing 3D holograms.

B. Holography principles

Holography is based on interference and diffraction, hence wave optics is used to study this phenomena as shall be discussed in the following section. It requires a setup that includes:

- A source of coherent light (a laser beam);
- Mirrors and lenses for light guiding;
- An object;
- A recording device (for instance, a photographic plate).

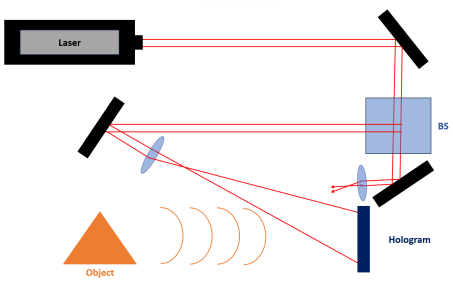

Figure 1. Setup used for hologram production.

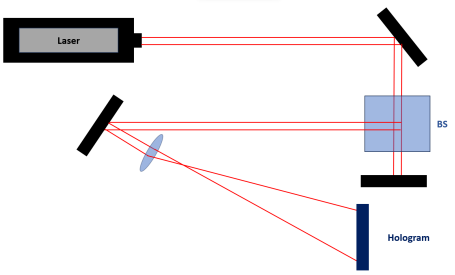

Figure 2. Setup used for image reconstruction.

Media are only sensitive to the intensity, thus to record the phase of the light field (which is encoded as intensity variations), it is used a complex setup [4]. As depicted in figure 1, light from the laser beam is split into two partial waves: the **reference wave** (the one that illuminates the medium directly) and the **object wave** that is reflected by the object. The interference of these two waves produces an interference pattern recorded in the medium, a **hologram**. On the other hand, to reconstruct the image, one illuminates the hologram with the reference wave, as shown in figure 2. Even though this image is virtual, it is indistinguishable from the original one.

This process presents several limitations. Firstly, this setup is extremely sensitive, since it is intended to produce clean and sharp interference fringes, thus requiring all path-length differences to be as stable as possible. In addition, recording a hologram is extremely time-consuming and the presence of the object is indispensable during that time.

Fortunately, these limitations were overcome with the introduction of Computer Generated Holography (CGH), which possesses various useful properties. For instance, it eliminates the need for an object and it provides the opportunity, with diffraction theory, to compute the interference pattern for an ideal wavefront which can be printed onto a mask or a film. These can be illuminated with a coherent source of light, producing an image. In section III, its potential is further explored; however, it opens a remarkable amount of possibilities, from the opportunity of recording objects that the setup of figure 1 cannot to the comfort of performing all these tasks solely with a computer.

C. Non-optical Holography

As previously stated, holography is not limited to optical waves, since Gabor's work was on electron waves. Holography covers a wide range of wavelengths, from x-ray (a probe to the atomic order of solids [5]) to microwave [6, 7].

Furthermore, holography can be applied to acoustics - **acoustic holography** [8] which enables sound waves of an

* goncalo.machado@tecnico.ulisboa.pt, manuelratola22@tecnico.ulisboa.pt, margarida.melo.pereira@tecnico.ulisboa.pt

[1] Light waves generated by a laser are extremely regular and highly monochromatic. Consequently, they are strongly coherent - the interference effects are very pronounced [1].

object to be generated.

Other examples include atomic holography (holograms in the atomic scale) as well as neutron beam holography to uncover the interior of solids.

D. Applications of holography

Holography possesses a wide range of applications, such as:

- Medical imaging (holographic display of patient's 3D data) [9–11];
- 3D Data storage[12];
- Fluid Mechanics with particle detection and 3D flow velocimetry [13];
- Security and authentication [14];
- Microscopic distribution of electromagnetic potentials (with electron holography) [15].

Just to name a few. It is, indeed, a widely used technique in industry, investigation and even art.

II. MATHEMATICAL DESCRIPTION

A. Wave Optics

In the previous section, we concluded that, since holography is based on interference and diffraction, the proper theory to treat it is the wave model. Light waves can be described either by an electric or a magnetic field, considering that they are perpendicular to each other and both are perpendicular to the wave propagation - light waves are transverse [16].

Physically, the only direct measurable quantity is the intensity, which is given by:

$$I = \epsilon_0 c < E^2 > \tag{1}$$

where <> denotes a time average over a period.

B. Interference and reconstruction

Interference is crucial in holography, thus let us dive into this concept. Given two monochromatic waves with amplitudes A_R and A_O (where R and O stand for reference wave and object wave), their intensity at the plane z=0 is given by:

$$\begin{aligned} I &= |A_R + A_O|^2 = |A_R|^2 + |A_O|^2 + A_R A_O^* + A_O A_R^* \\ &= I_R + I_O + 2\sqrt{I_R I_O}\cos[arg(A_R) - arg(A_O)] \end{aligned}$$

Assuming that on that plane there is a transparency, its transmittance is proportional to I, thus containing information regarding the phase of both waves due to the cosine argument.

Now, we are in position, as described in the previous section, to produce an image with our hologram (the transparency). By illuminating it with the reference wave, one obtains a wave with an amplitude in the plane z=0 equal to:

$$A = tA_R \propto A_R I_R + A_R I_O + I_R A_O + A_R^2 A_O^* \tag{2}$$

Analyzing it, one can easily say that the third term is the object wave multiplied by I_R, which, if the latter is independent of x and y constitutes our desired reconstructed wave multiplied by I_R. Thus, it is now needed to separate this wave from the others [17].

A method to achieve this is to ensure that the four waves vary at well-separated spatial frequencies, hence having well-separated directions. Considering $A_O = f(x,y)\exp(-ikx\sin\theta)$ and imposing that it varies slowly (so that its maximum spatial frequency ν_s corresponds to an angle $\theta_s = \sin^{-1}(\lambda\nu_s) \ll \theta$), it is possible to rewrite equation 2 as:

$$A \propto I_R + |f(x,y)|^2 + \sqrt{I_R} f(x,y) e^{-g} + \sqrt{I_R} f^*(x,y) e^{g} \tag{3}$$

where g = $ikxsin\theta$.

The third term is a replica of our object wave that arrives from a direction of θ, whereas the fourth term is known as the conjugate object wave and deflects into -θ direction. The first term is a plane wave propagating in the z-direction and, finally, the second term is the ambiguity term - it is a nonuniform plane wave in directions within a cone of $2\theta_s$ around the z-axis. If we satisfy the condition $\theta > 3\theta_s$, the object wave is reconstructed unambiguously. Alternatively, one can impose that the intensity of the reference wave is much greater than the one of the object wave [17].

C. Fourier Optics

Since holography demands a wave treatment of light, Fourier Optics plays a critical role in our work, since it is the mathematical tool used to calculate and analyze light propagation considering its wave nature. We proposed to study, in a simulation environment, the role that devices whose purpose is to change a field's phase (such as a Spatial Light Modulator - SLM) play in holography [17, 18].

Amplitude computations are fairly easy when using Fourier Optics since one must perform the following steps:

1. Apply a spatial Fourier Transform to the amplitudes;
2. Multiply the given result by the transfer function;
3. Apply an inverse spatial Fourier transform if the results are needed in real space.

Regarding free space, the transfer function for a wave propagating in z-direction with a wavelength λ is given by equation 4, whereas for a thin lens is described by equation 5. The Spatial Light Modulator transfer function is presented in the following sections

$$H(\nu_x, \nu_y) = \exp\left(2\pi i d\sqrt{\frac{1}{\lambda^2} - \nu_x^2 - \nu_y^2}\right) \tag{4}$$

$$t_{lens} = \exp\left(-i\frac{\pi}{\lambda f}(x^2 + y^2)\right) \tag{5}$$

III. COMPUTER GENERATED HOLOGRAPHY

A. Generation methods

Computer generated holography surpasses the limitations imposed by traditional optical recording methods, revolutionizing hologram production. It comes, however, with the

caveat of high computational demand, requiring significant processing power and time, especially for complex scenes or high-resolution holograms. The main approaches for reaching faster calculation times can be divided into Wavefront-based (Point, Polygon and Layer) (see Fig.3) and Ray-based methods [19, 20]

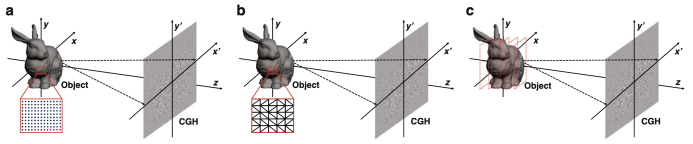

Figure 3. Wavefront-based CGH calculation methods. a) Point-based method; b) polygon-based method; c) layer-based method.

1. *Point-based*

In this model, 3D objects are discretized into a dense collection of points, where each point is a self-emitting primitive. The hologram is formed when superposing the fringe patterns (FPs) of all primitives in the hologram plane. The calculations involved are fairly simple, however, due to the density of the points needed, the computational burden can reach the limits of modern computers.

Literature proposed techniques to circumvent these limitations which are based on the idea of calculating and storing FPs in advance. The first technique proposed in [21], used Look-Up-Tables (LUTs), pre-computed and stored segments of the calculations conducted during the recording process. Afterwards, CGHs are created by sequentially accessing and combining the pre-stored FPs. Other methods rework the idea of LUTs in order to improve added storage constraints. N-LUTs [22] first divide objects into 2D slices and only the FP of the center object point in each sliced plane is pre-calculated and stored. Other methods include split-LUT (S-LUT) [23], and compressed-LUT (C-LUT) [24].

An alternative method of speeding up calculations is a wavefront-recording plane (WRP) [25] where a virtual place is placed between the object and the hologram plane. The points are initially assessed within the WRP, followed by the propagation of the WRP content across the hologram plane. This approach reduces computational burden by utilizing smaller-sized FPs on the WRP compared to the larger size of the CGH. This method has been combined with a new approach WASABI [25, 26] to further increase these speeds.

2. *Polygon-based*

In this method, instead of dividing the object into points, these are substituted by fewer polygon shapes (e.g., triangle) [27]. In the same way, these are self-emitting and the resulting hologram is a sum of the 2D surfaces. Since it requires fewer objects, it is less heavy than the point-cloud structure. This method also adds the advantage of easily combining with rendering algorithms of computer graphics to add shaders and texture maps [28]. It is less efficient for more complex scenes requiring a high number of polygons to achieve the required resolution. Despite various advancements in polygon-based methods aimed at circumventing intricate computations, these approaches often necessitate additional computations for diffusion and texture inclusion, thereby contributing to time-consuming processes.

3. *Layer-based*

Layer-based methods involve partitioning the 3D object into multiple layers aligned parallel to the hologram plane [29]. Each layer functions as an independent light-emitting primitive and is propagated towards the hologram plan. Utilizing Fresnel diffraction, individual sub-holograms are computed for each layer. Finally, CGHs are derived by combining all these computed sub-holograms. However, achieving seamless depth perception within the scene can result in a high number of layers to minimize noticeable visual discontinuities. This method has recently been combined with LUTs [30] to reduce computation time without compromising resolution.

4. *Ray-Based*

This method distinguishes itself from the previously explored in this section since the objects are no longer self-emitting, instead light rays propagate from a virtual viewpoint interacting with the objects in the 3D scene [19]. These methods are computationally intensive but provide accurate and realistic holographic renderings by simulating the behavior of light rays.

In [31], a light-ray sampling plane (RS) is positioned between the virtual camera and the objects in the scene. The captured light rays are transformed into wavefronts through Fourier transforms, framing this as a hybrid approach. These wavefronts are subsequently propagated to the CGH plane. The suggested technique applies to both virtual and real objects, encompassing computer-generated imagery as well as multi-view image data captured by a camera array. Contrary to other ray-based approaches, the resolution of the images obtained is not dependent on location, preserving long-distance resolution. Moreover, this method can replicate angular reflection characteristics, like glossy or metallic attributes, generating more realistic rendering techniques.

Research into the use of multiple GPUs is underway [32] in order to realize a real-time holographic display system.

B. Reconstruction methods

As with generation methods, reconstruction methods can be computationally heavy and different approaches have been developed to address this issue.

For this step, the basis is light propagation, expressed numerically through scalar diffraction theory [19], often approximated through bidimensional Discrete Fourier Transforms (2D DFT). Two reconstruction techniques that are frequently employed are the Fresnel transformation and the Angular Spectrum Method (ASM).

In the Fresnel transformation, the Fresnel approximation is applied to calculate the reconstructed wavefield at the reconstruction plane with one 2D DFT. To avoid performing an approximation, the ASM method can be applied instead, with the trade-off that two Fourier Transforms are needed, increasing the computational load.

For reconstructions that require higher computational resources, software and hardware modifications have been proposed and implemented. One reconstruction software [33] specialized in microscopy holograms is able to render real-time interferograms through parallel computing in GPUs. Another example is the Computational Wave Optics library for C++ (CWO++) [34], this software library not only leverages CPU power but also harnesses the GPU for accelerated calcula-

tions. Both mentioned software implementations are actively maintained and publicly accessible. Hardware developments include general-purpose GPU clusters [35], able to render images at 30 frames-per-second, or smaller specialized solutions [36] like the recently proposed HORN-8 system [37, 38].

C. Speckle Suppression

Since coherent light is used during hologram recording and reconstruction, it is necessary to deal with speckle noise, constructive and destructive interference patterns, resulting in the characteristic granular appearance. This adversely impacts the quality of the reconstructed image and active research is needed to address this issue.

The methods that tackle this issue can either be in the hologram generation process or in the reconstruction process. Regarding the first, the CGH algorithm can be divided into two categories: iterative (Gerchbert-Saxton algorithm is the most famous) and non-iterative (the multi-random phase method and multiple fractional Fourier transform method). For the latter, the reduction of light source coherence (which can be achieved with a random laser) is an example, even though it presents several drawbacks, with impacts on the sharpness and contrast of the reconstructed image, demanding a compromise [39].

IV. SPATIAL LIGHT MODULATORS (SLM)

Spatial light modulation is a well-established modern method of light shaping through the use of CGHs with a wide range of applications. SLM devices are able to manipulate various light properties such as amplitude, phase, and polarization. Essentially, these are devices composed of liquid crystal (LC) filled cells that can be controlled individually [40].

A. Liquid crystals

Liquid crystals (LC) are composed of elongated molecules which exhibit distinct behaviors, categorizing this material into an intermediate state of matter between liquid and solid. Under specific conditions, these molecules will align under different orientations while maintaining their fluid nature. Depending on their molecular arrangement, LC can be categorized as nematic, smetic, or cholesteric (figure 4).

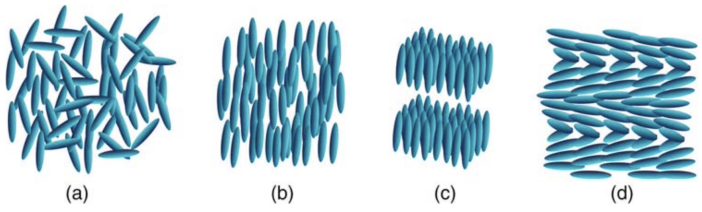

Figure 4. Schematic representation of different molecular alignments in a liquid crystal: (a) liquid, (b) nematic, (c) smetic, and (d) cholestric.

In nematic LCs, the molecules are randomly positioned but aligned in a unified direction, these are characterized by one symmetry axis called the director [41]. This axis can be reoriented with an external field, such as an electric, optical or magnetic fields.

Due to their asymmetric structure, LC molecules possess different optical properties along different axes, resulting in birefringent behavior. Variations in the refractive index are predominant along the long axis of the molecules. This is termed the "slow axis", since light traveling through this direction experiences the slowest refractive index.

B. Spatial light modulator technology

Commercial SLMs are usually electro-optical, meaning that the orientation of the crystal structure is controlled with an electrical field. They can be transmissive or reflective, the former utilizing liquid-crystal displays (LCDs) and the latter liquid crystal on silicon (LCoS) displays.

The devices are calibrated so that the orientation of the LCs in each pixel depends on the magnitude of the voltage applied. Typically, this voltage is controlled by the gray-scale information of a provided image (usually 8-bit encoding). Therefore, the resulting $2\pi/256$ phase increments can be encoded at each pixel on the LC display by displaying an image, provided by an associated computer.

C. Limitations and current research

Despite their ease of use and popularity, these devices face some limitations. A challenge with this technology is pixelation, resolution is limited by the number of pixels and their spacing. This issue is especially relevant for Transmissive SLMs, since LCoS-SLMs achieve higher pixel density.

Furthermore, 5% to 20% of light remains "undiffracted" since it doesn't interact with the CGH [19]. If this component isn't filtered out, it can lead to undesired interference patterns.

Research to address these limitations is still underway. Alternative methods like light valve modulators (OASLM) [42], thermal or thermo-optical control of the LC layer and dielectric metasurfaces [43] can be promising candidates to address issues like pixelization.

D. AI-assisted CGH

The complexity of computer generated holography leads itself to the need for various strategies in simplifying and improving these methods. Thus, artificial intelligence techniques are more and more relevant, specifically when associated to the use of SLMs. There are many approaches to reaching the improvement needed to obtain useful CGH methods.

Before the SLM can be employed it goes through a process of calibration [40]. Various methods to perform this calibration have been proposed in Literature, more intensive methods can benefit from the use of Machine Learning in order to streamline this process.

A more obvious use for these machine-learning (ML) algorithms is in the generation process of the phase-masks that are implemented by the SLM. These algorithms compute the most suitable phase and amplitude distributions for the SLMs to generate high-quality holograms. In [44] deep neural networks (DNNs) were used to improve the phase retrieval in measurements prone to strong artifacts. The combination of a Gerchberg-Saxton (GS) algorithm and DNNs leading to improved reconstructions. Another example is the proposal for the use of deep convolutional neural networks (CNNs) allied to a GS algorithm to shape a laser beam and electron beam [45].

Here ML is introduced to mitigate the non-linear distortions and improve the laser pulse shaping results.

Besides aiding in the generation of phase masks, many of these algorithms were designed with the intention of reducing Speckle and other noise based effects. Alternative methods where ML is employed are presented in [46–48].

V. 3D HOLOGRAPHY

Ever since the first original observations by Sir Charles Wheatstone were presented to the Royal Society in London in 1838 [49], following the construction of the first stereoscope in 1832, achieving true three-dimensional displays has been an important goal in optics and other fields.

Extensive research has been done in the past decades reaching various solutions (stereoscopy, auto-stereoscopy, volumetric display) [50]. However, most of these advancements have been based on the original stereoscopic idea and are limited to a two-view system, unable to achieve full-parallax [51], resulting in important limitations. These displays often come with restricted viewing angles, causing discomfort and visual inconsistency beyond these angles. Depth resolution might not be as precise as natural vision, leading to challenges in perceiving subtle depth cues. Prolonged use can induce nausea, eye strain and fatigue due to needed adjustment for convergence and focus.

Recent developments have shifted focus to new CGH technologies, with the objective of providing full-parallax.

3D Holography using SLM manipulates beams of light to create 3D imaging without the need for any special glasses, where SLMs play a big role due to their capacity to modulate the phase. There are two principal ways to implement 3D Holography: Single SLM and Dual SLM [52]. Using a Single SLM, Phase-only modulation (specified in Section VI) is the most interesting way to generate 3D Holograms. It is the simplest and cheapest way to create 3D images however it requires more computational power and can introduce noise. In a dual SLM system, one is responsible for the amplitude modulation and the other for the phase modulation. However, this system is more expensive and requires the perfect alignment between the two SLMs. As so, creating live and high-quality holograms has some obstacles, namely the lack of fast algorithms that can generate high-quality holograms from 3D point clouds, or light fields in real-time [53].

VI. BEAM SHAPING

This section will focus on producing different types of beams (for example, vortex beams) using holography.

A. Phase modulation and transfer function

Our main goal is to start from a given optical field and create an arbitrary optical field by using phase-only devices (i.e. SLM). Analytically, this can be made by the use of a transfer function t. Given an arbitrary optical field $u_1 = Ae^{i\phi_1}$ and a desired field which has the following form, $u_2 = Be^{i\phi_2}$, the transfer function associated with this transformation will be given by (6).

$$t = \frac{A}{B} e^{i(\phi_2 - \phi_1)} \tag{6}$$

During this work, it will always be considered $A = B$ as we are interested in the study of the SLM phase modulation properties. However, it is possible to modulate the amplitude and the phase of a beam using a phase-only device using diverse techniques described in [40]. Then, for a phase-only hologram, the programmed phase is just $mod[\phi_2 - \phi_1, 2\pi]$. If we choose the input beam phase flat or constant, it simplifies to $mod[\phi_2, 2\pi]$. However, using a phase-only beam has its restrictions because the desired optical field is only created in the far field. Experimentally, putting the detector (a camera or a screen) very far away from the SLM device is not practical, so usually a thin lens is placed next to the the SLM at a distance f, which corresponds to the focal distance of the lens. The detector is placed at a focal distance f from the lens as shown in 5.

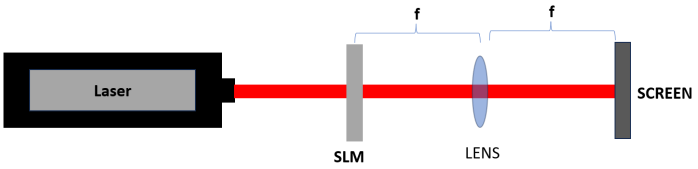

Figure 5. Experimental Setup used for Beam shaping and simulations.

B. Generation of Vortex beam

As an application example of a phase-only modulation using an SLM, it can be considered a setup where we consider as an input a Gaussian beam [40]. With the SLM, is imposed a varying azimuthal phase. This setup creates a Vortex Beam. These beams have the mathematical form of (7).

$$E(\varphi) = E_0 e^{il\varphi} \tag{7}$$

where $\varphi = \arctan\left(\frac{y}{x}\right)$ in the XY-plane and is the azimuthal angle, l is the topological charge of the vortex beam (i.e number of twists the light does in one wavelength) and is any integer value and E_0 is the Beam part that is independent of the azimuthal angle. These beams are called vortex beams because of the discontinuity at $\varphi = 0$ which produces null intensity at the origin.

Figure 6. Representation of vortex beam. The middle image is the representation of the phase difference between the different parts of the beam, right is an XY-plane slice [54].

Therefore, a phase modulation of a Gaussian Beam into a Vortex beam can be easily done by encoding an azimuthal variation using an SLM with the following expression:

$$\Phi_{SLM} = mod[l\varphi, 2\pi] \tag{8}$$

For this work, simulations were made using the setup 5 to demonstrate the effectiveness of this method to generate vortex beams. The results are in section VII.

C. Gerchbert-Saxton algorithm

Although the utility and effectiveness of the previous method to create a vortex beam, it is now needed a systematic

way to know the Φ_{SLM} which is associated with any arbitrary output. That is done iteratively with the Gerchbert-Saxton (GS) algorithm. The GS algorithm is an iterative numerical method used in the field of optics for determining the phase of a complex-valued wavefield from intensity measurements alone. It was introduced by R. W. Gerchberg and W. O. Saxton in 1972. The algorithm is particularly useful in situations where direct phase measurement is challenging or impossible, and only the intensity pattern can be measured. It is widely applied in various fields, including X-ray crystallography, electron microscopy, and coherent imaging. The GS algorithm can be summarized by the following pseudocode:

1. Initialization of a complex field A with the amplitude and phase of the wanted output.
2. Creation of an intermediate complex field B that has the amplitude from the source and the phase obtained from the current estimate A.
3. Creation of an intermediate complex field D with the amplitude from the output and the phase obtained from the Fourier transform of B.
4. Finally, A is updated with the inverse Fourier transform of D.
5. Iteration of the steps 2-4 until a predetermined number of iterations.
6. The final output of the algorithm is the phase of the complex field A, which is considered to be the retrieved phase.

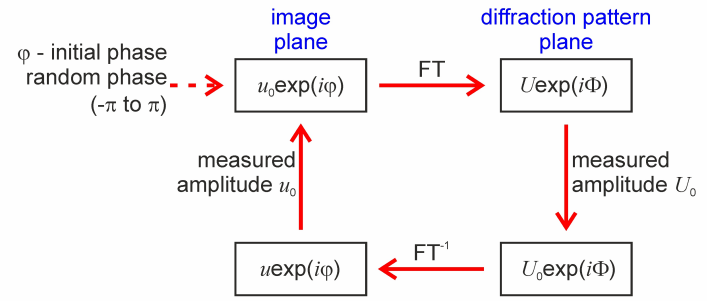

Figure 7. Gerchberg-Saxton algorithm [55].

The simulations regarding the algorithm are presented in section VII.

VII. SIMULATIONS AND RESULTS

A. Generation of Vortex beam

A Python code (Appendix A) was implemented to simulate the generation of a Vortex Beam with an SLM. The conditions for the implementation of this code were described in section VI and it was used the setup from 5. To simulate the Gaussian Beam, a 2D mesh grid was created where the intensity of each pixel was given by (9)

$$E = Ae^{-(x^2+y^2)/W_0^2} \tag{9}$$

which corresponds to the expression of a Gaussian Beam with $z = 0$, where $x^2+y^2 = \rho^2$ which is the distance from the center $(x, y) = (0, 0)$. Then, a Fourier propagation was made to propagate the beam to the SLM. The transfer function $e^{i\Phi_{SLM}}$ was applied with Φ_{SLM} described by (8). Finally, the far field was obtained by using the transfer function of a thin lens with focal distance $f = 0.3m$. The results of the simulations are presented below. Notice that the scales are different in some plots to analyze them better. Firstly we plot the input Gaussian beam used 8, with $A = 1V/m$, $W_0 = 5 * 10^{-4}m$, $\lambda = 0.6328 * 10^{-6}m$. The scale at right describes the intensity and it is measured in W/m^2.

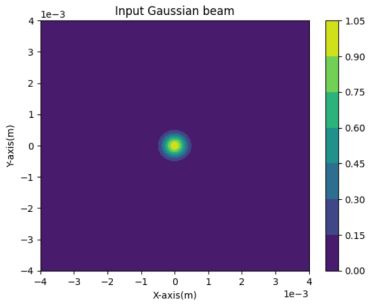

Figure 8. Initial Gaussian Beam.

Then, we plot the vortex obtained after the SLM and observed in the far field for different values of topological charge ($l = 1$ and $l = 3$).

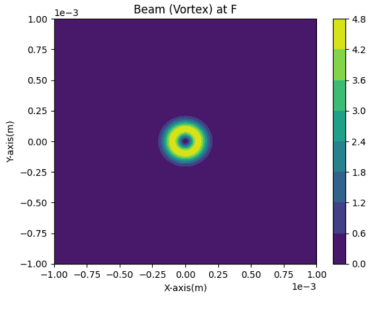

Figure 9. Vortex Beam formed after SLM with $l = 1$.

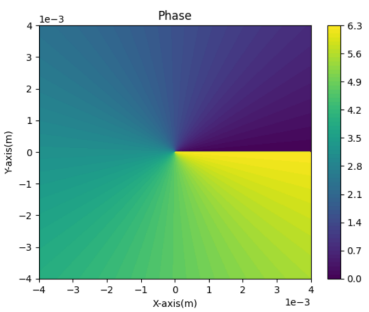

Figure 10. SLM phase with $l = 1$.

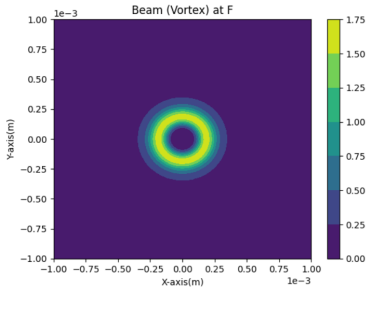

Figure 11. Vortex Beam formed after SLM with $l = 3$.

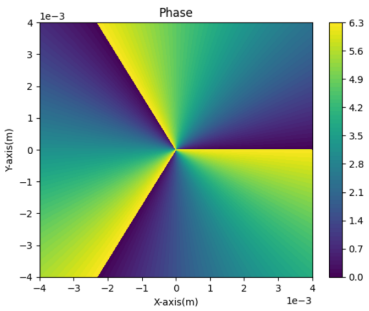

Figure 12. SLM phase with $l = 3$.

The results of the simulations are coherent with the theory and indeed it is possible with a phase-only device to generate a Vortex Beam with a Gaussian Beam as an input. However, it is visible that some undesired rings are formed in 11 and 12. This happens since the simulations use a pure azimuthal phase without a radial intensity dependence, which does not maintain its form while traveling in free space because it is not an eigenmode of the free space Maxwell equation. Also, the vortex beam is affected by the change of the topological charge l: $l = 3$ beam is larger however the intensity of the main ring decreases.

B. Phase determination using Gerchbert-Saxton algorithm

Some simulations were made to test the iterative algorithm that is used to determine the SLM phase for any hologram.

Firstly, a simple input was chosen, and the number of iterations for a good convergence was tested. The plots for 5, 30 and 100 iterations are shown in 13, 14, and 15, respectively. The recovered image was obtained using the inverse Fourier transform of $e^{-i\phi_{ret}}$, where ϕ_{ret} is the retrieved phase. From now on, the x and y axis in the graphs represent the number of pixels of the image.

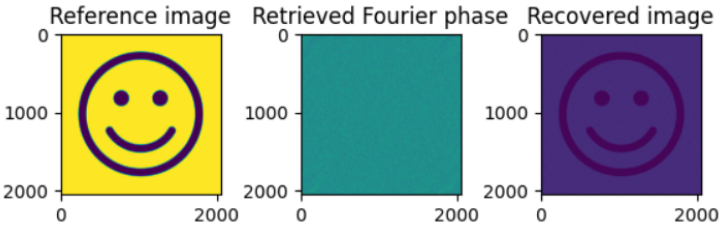

Figure 13. GS algorithm applied to a simple reference image with 5 iterations.

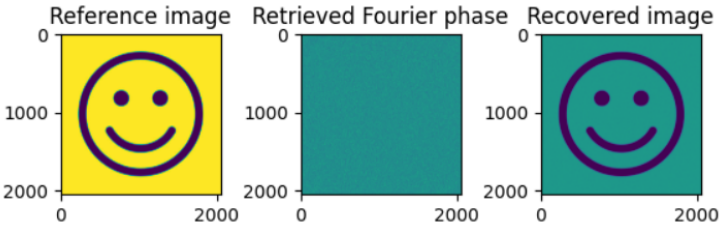

Figure 14. GS algorithm applied to a simple reference image with 30 iterations.

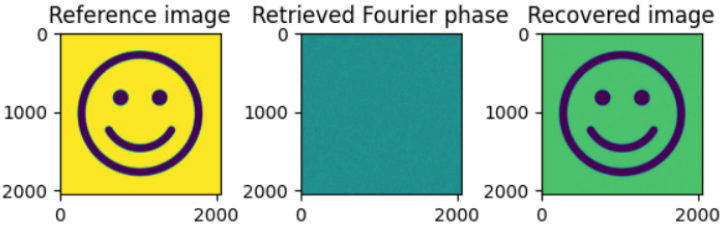

Figure 15. GS algorithm applied to a simple reference image with 100 iterations.

As expected, a larger number of iterations implies a better quality in the recovered image. However, many iterations also imply the necessity of a larger computational power. For 30 iterations, the reference image is visible with sufficient clarity. As such, from now on, 30 iterations will be the reference number of iterations done in the next simulations. Secondly, the GS algorithm was applied to a more complex image 16. As expected the results maintained their quality which confirms the quality and effectiveness of this algorithm.

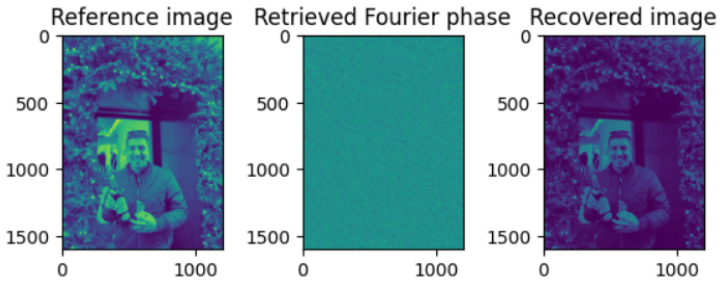

Figure 16. GS algorithm applied to a more complex reference image with 30 iterations.

C. Use of the Retrieved Phase in a Gaussian Beam

Finally, the Retrieved phase was tested in the SLM, by substituting Φ_{SLM} for the Phase obtained with the GS algorithm. The methods and scenario used in the simulations were the same as in subsection VII A. The results obtained are presented in fig.17.

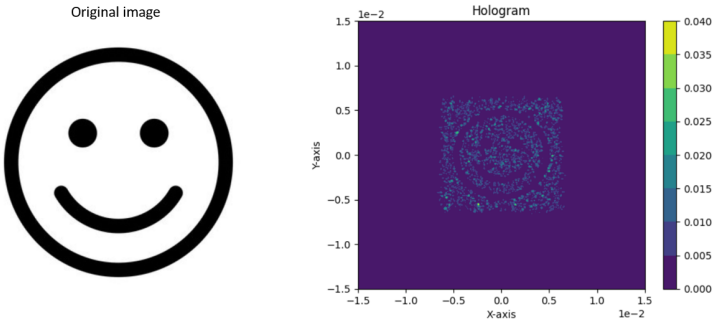

Figure 17. Effect of the SLM in a Gaussian beam using the retrieved phase of GS algorithm

The Hologram obtained seems very close to the original image, which is expected and confirms the fact that it is possible to create any hologram by just changing the phase of the input beam, in this case, a Gaussian beam.

VIII. CONCLUSION

Our work was centered on holography and it was centered on the applications of Spatial Light Modulators (SLM) in simulation. It was a challenge proposed by Dr. Pablo San Miguel, who, at VOXEL in IST, works with this device, which is state-of-the-art. Hence, this work provided us the opportunity to contact the frontiers of research that are being currently developed at VOXEL and throughout the world.

We first presented an overview of holography, discussing its principles, and introducing wave optics as the mathematical tool to understand this concept. Holograms were first produced with a highly sensitive setup (figure 1) and, then, due to its limitations, Computer Generated Holography took the spotlight. It possesses various advantages regarding the traditional procedure, such as eliminating the need for an object or the comfort of producing a hologram solely with a computer that afterward could be printed into a mask and used.

Different reconstruction and generation methods employed in Computer Generated Holography were reviewed as well as the features, limitations, and current research of Spatial Light Modulators, including the use of Machine Learning with this technology.

Regarding the code developed, we implemented a simulation that is based on the concept of SLM: changing the phase of the wave. With this, we generated a vortex beam from a Gaussian beam. These beams have several applications, such as atomic and molecular excitation, optical vortex coronagraphs, nano-lithography, laser cutting and machinery, data transfer, and optical tweezers manipulations. Furthermore, using the Gerchbert-Saxon algorithm, we determined the SLM phase for any hologram and, with that, reconstructed different images.

For future work, we intend to use our *software* at VOXEL's facilities to verify in the laboratory that our simulation results match with the observed during the experience. This part will be developed after the oral presentation under the supervision

of Dr. Pablo San Miguel and it aims to compare the simulation and experience results.

ACKNOWLEDGEMENTS

We extend our sincere gratitude to Dr. Pablo San Miguel and Engineer Rafael Almeida for their invaluable support in providing clarity and addressing our inquiries. Their unwavering availability proved to be instrumental in the successful attainment of our research outcomes.

[1] D. Gabor, W. E. Kock, and G. W. Stroke, "Holography: The fundamentals, properties, and applications of holograms are reviewed.," *Science*, vol. 173, no. 3991, pp. 11–23, 1971.

[2] G. Tricoles, "Computer generated holograms: an historical review," *Applied optics*, vol. 26, no. 20, pp. 4351–4360, 1987.

[3] W. Osten, A. Faridian, P. Gao, K. Körner, D. Naik, G. Pedrini, A. K. Singh, M. Takeda, and M. Wilke, "Recent advances in digital holography," *Applied optics*, vol. 53, no. 27, pp. G44–G63, 2014.

[4] D. P. Kelly, B. M. Hennelly, N. Pandey, T. J. Naughton, and W. T. Rhodes, "Resolution limits in practical digital holographic systems," *Optical Engineering*, vol. 48, no. 9, pp. 095801–095801, 2009.

[5] G. Faigel, G. Bortel, C. Fadley, A. Simionovici, and M. Tegze, "Ten years of x-ray holography," *X-Ray Spectrometry: An International Journal*, vol. 36, no. 1, pp. 3–10, 2007.

[6] A. Anderson, "Microwave holography," in *Proceedings of the Institution of Electrical Engineers*, vol. 124, pp. 946–962, IET, 1977.

[7] W. E. Kock and W. E. Kock, "Microwave holography," *Engineering Applications of Lasers and Holography*, pp. 179–223, 1975.

[8] R. K. Mueller, "Acoustic holography," *Proceedings of the IEEE*, vol. 59, no. 9, pp. 1319–1335, 1971.

[9] P. Greguss, "Holographic displays for computer assisted tomography," *Journal of Computer Assisted Tomography*, vol. 1, no. 2, pp. 184–186, 1977.

[10] E. Bruckheimer, C. Rotschild, T. Dagan, G. Amir, A. Kaufman, S. Gelman, and E. Birk, "Computer-generated real-time digital holography: first time use in clinical medical imaging," *European Heart Journal-Cardiovascular Imaging*, vol. 17, no. 8, pp. 845–849, 2016.

[11] A. Haleem, M. Javaid, and I. H. Khan, "Holography applications toward medical field: An overview," *Indian Journal of Radiology and Imaging*, vol. 30, no. 03, pp. 354–361, 2020.

[12] L. Hesselink, S. S. Orlov, and M. C. Bashaw, "Holographic data storage systems," *Proceedings of the IEEE*, vol. 92, no. 8, pp. 1231–1280, 2004.

[13] J. Katz and J. Sheng, "Applications of holography in fluid mechanics and particle dynamics," *Annual Review of Fluid Mechanics*, vol. 42, pp. 531–555, 2010.

[14] I. M. Lancaster, "Future for security applications of optical holography," in *International Conference on Applications of Optical Holography*, vol. 2577, pp. 71–76, SPIE, 1995.

[15] A. Tonomura, "Applications of electron holography," *Reviews of modern physics*, vol. 59, no. 3, p. 639, 1987.

[16] U. Schnars, C. Falldorf, J. Watson, W. Jüptner, U. Schnars, C. Falldorf, J. Watson, and W. Jüptner, *Digital holography*. Springer, 2015.

[17] B. E. Saleh and M. C. Teich, *Fundamentals of photonics*. john Wiley & sons, 2019.

[18] R. P. Encyclopedia, "Fourier optics," 2024. Accessed: 04/01/2024.

[19] R. Corda, D. Giusto, A. Liotta, W. Song, and C. Perra, "Recent advances in the processing and rendering algorithms for computer-generated holography," *Electronics*, vol. 8, no. 5, 2019.

[20] D. Pi, J. Liu, and Y. Wang, "Review of computer-generated hologram algorithms for color dynamic holographic three-dimensional display," *Light: Science & Applications*, vol. 11, no. 1, p. 231, 2022.

[21] M. Lucente, ""interactive computation of holograms using a look-up table"," *Journal of Electronic Imaging*, vol. 2(1), 09 1995.

[22] S.-C. Kim and E.-S. Kim, "Effective generation of digital holograms of three-dimensional objects using a novel look-up table method," *Applied optics*, vol. 47, pp. D55–62, 08 2008.

[23] Y. Pan, X. xu, S. Solanki, X. Liang, R. Tanjung, C. Tan, and T.-C. Chong, "Fast cgh computation using s-lut on gpu," *Optics express*, vol. 17, pp. 18543–55, 10 2009.

[24] C. Gao, J. Liu, X. Li, G. Xue, J. Jia, and Y. Wang, "Accurate compressed look up table method for cgh in 3d holographic display," *Optics Express*, vol. 23, p. 33194, 12 2015.

[25] T. Shimobaba, N. Masuda, and T. Ito, "Simple and fast calculation algorithm for computer-generated hologram with wavefront recording plane," *Optics letters*, vol. 34, pp. 3133–5, 10 2009.

[26] T. Shimobaba and T. Ito, "Fast generation of computer-generated holograms using wavelet shrinkage," *Opt. Express*, vol. 25, pp. 77–87, Jan 2017.

[27] K. Matsushima and S. Nakahara, "Extremely high-definition full-parallax computer-generated hologram created by the polygon-based method," *Applied optics*, vol. 48, pp. H54–63, 12 2009.

[28] W. Lee, D. Im, J. Paek, J. Hahn, and H. Kim, "Semi-analytic texturing algorithm for polygon computer-generated holograms," *Optics express*, vol. 22, pp. 31180–91, 12 2014.

[29] M. Bayraktar and M. Özcan, "Method to calculate the far field of three-dimensional objects for computer-generated holography," *Applied optics*, vol. 49, pp. 4647–54, 08 2010.

[30] Y. Li, D. Wang, N.-N. Li, and Q.-H. Wang, "Fast hologram generation method based on the optimal segmentation of a sub-cgh," *Optics Express*, vol. 28, 10 2020.

[31] K. Wakunami and M. Yamaguchi, "Calculation for computer generated hologram using ray-sampling plane," *Optics express*, vol. 19, pp. 9086–101, 05 2011.

[32] H. Sato, T. Kakue, Y. Ichihashi, Y. Endo, K. Wakunami, R. Oi, K. Yamamoto, H. Nakayama, T. Shimobaba, and T. Ito, "Real-time colour hologram generation based on ray-sampling plane with multi-gpu acceleration," *Scientific Reports*, vol. 8, 01 2018.

[33] M. Atlan, "Ultrahigh-throughput rendering of digital holograms," p. DM5F.4, 01 2018.

[34] T. Shimobaba, J. Weng, T. Sakurai, N. Okada, T. Nishitsuji, N. Takada, A. Shiraki, N. Masuda, and T. Ito, "Computational wave optics library for c++: Cwo++ library," *Computer Physics Communications*, vol. 183, pp. 1124–1138, May 2012.

[35] H. Niwase, N. Takada, H. Araki, Y. Maeda, M. Fujiwara, H. Nakayama, T. Kakue, T. Shimobaba, and T. Ito, "Real-time electroholography using a multiple-graphics processing unit cluster system with a single spatial light modulator and the infiniband network," *Optical Engineering*, vol. 55, 09 2016.

[36] T. Shimobaba, T. Kakue, and T. Ito, "Review of fast algorithms and hardware implementations on computer holography," *IEEE Transactions on Industrial Informatics*, vol. 12, pp. 1–1, 01 2015.

[37] T. Sugie, T. Akamatsu, T. Nishitsuji, R. Hirayama, N. Masuda, H. Nakayama, Y. Ichihashi, A. Shiraki, M. Oikawa, N. Takada, Y. Endo, T. Kakue, T. Shimobaba, and T. Ito, "High-performance parallel computing for next-generation

holographic imaging," *Nature Electronics*, vol. 1, pp. 254–259, Apr. 2018.
[38] T. Nishitsuji, Y. Yamamoto, T. Sugie, T. Akamatsu, R. Hirayama, H. Nakayama, T. Kakue, T. Shimobaba, and T. Ito, "Special-purpose computer horn-8 for phase-type electroholography," *Optics Express*, vol. 26, pp. 26722–26733, Oct. 2018.
[39] N.-N. Li, C. Chen, B. Lee, D. Wang, and Q.-H. Wang, "Speckle noise suppression algorithm of holographic display based on spatial light modulator," *Frontiers in Photonics*, vol. 2, p. 10, 2022.
[40] C. Rosales-Guzmán and A. Forbes, "How to shape light with spatial light modulators," 2017.
[41] U. Efron, *Spatial light modulator technology : materials, devices, and applications*. No. v. 47 in Optical engineering, Marcel Dekker, 1995.
[42] P. Shrestha, Y. Chun, and D. Chu, "High resolution optically addressed spatial light modulator based on zno nanoparticles," *Light: Science Applications*, vol. 4, 03 2015.
[43] A. C. Overvig, S. Shrestha, S. C. Malek, M. Lu, A. Stein, C. Zheng, and N. Yu, "Dielectric metasurfaces for complete and independent control of the optical amplitude and phase," *Light: Science amp; Applications*, vol. 8, Oct. 2019.
[44] I. Kang, F. Zhang, and G. Barbastathis, "Phase extraction neural network (phenn) with coherent modulation imaging (cmi) for phase retrieval at low photon counts," *Optics Express*, vol. 28, 06 2020.
[45] C. Xu, E. Bründermann, M. Nasse, A. Santamaría García, C. Sax, C. Widmann, and A.-S. Muller, "Machine learning based spatial light modulator control for the photoinjector laser at flute," 10 2021.
[46] D. Mikhaylov, B. Zhou, T. Kiedrowski, R. Mikut, and A. Lasagni, "High accuracy beam splitting using spatial light modulator combined with machine learning algorithms," *Optics and Lasers in Engineering*, vol. 121, pp. 227–235, 04 2019.
[47] J. Amari, J. Takai, and T. Hirano, "Highly efficient measurement of optical quadrature squeezing using a spatial light modulator controlled by machine learning," *Opt. Continuum*, vol. 2, pp. 933–941, 2023.
[48] D. Lin, D. Li, Y. Cui, T. Zhang, F. Meng, X. Zhao, J. Ding, and S. Liang, "Machine learning-based error compensation for high precision laser arbitrary beam splitting," *Optics and Lasers in Engineering*, vol. 160, p. 107245, 01 2023.
[49] C. Wheatstone, "Contributions to the physiology of vision. part the first. on some remarkable, and hitherto unobserved, phenomena of binocular vision," *Philosophical Transactions of the Royal Society*, vol. 128, pp. 371–394, 1838.
[50] L. Yang, H. Dong, A. Alelaiwi, and A. El Saddik, "See in 3d: state of the art of 3d display technologies," *Multimedia Tools and Applications*, vol. 75, 12 2016.
[51] N. Holliman, N. Dodgson, G. Favalora, and L. Pockett, "Three-dimensional displays: A review and applications analysis," *Broadcasting, IEEE Transactions on*, vol. 57, pp. 362 – 371, 07 2011.
[52] W. Zaperty, T. Kozacki, and M. Kujawinska, "Multi-slm color holographic 3d display based on rgb spatial filter," *Journal of Display Technology*, vol. PP, pp. 1–1, 10 2016.
[53] S.-F. Lin and E.-S. Kim, "Single slm full-color holographic 3-d display based on sampling and selective frequency-filtering methods," *Opt. Express*, vol. 25, pp. 11389–11404, May 2017.
[54] D. Gozzard, "Twisting light: Creating an optical vortex," Dec. 2023.
[55] W. contributors, "Gerchberg–saxton algorithm," 2024. Accessed: 04/01/2024.

Appendix A: Code

In this project, the results were obtained using a code developed in the Python programming language. All the code for the simulations can be found on GitHub:Python Simulations.